

Affinity Distributions of a Molecularly Imprinted Polymer Calculated Numerically by the Expectation-Maximization Method

Brett J. Stanley

Department of Chemistry, California State University, San Bernardino, California 92407

Pawel Szabelski

*Department of Theoretical Chemistry, Maria Curie-Skłodowska University,
20-031 Lublin, Poland,*

Y.-B. Chen

Fox Chase Cancer Center, Biotech Facility, Philadelphia, Pennsylvania 19111

Borje Sellergren

*Department of Inorganic Chemistry and Analytical Chemistry,
Johannes Gutenberg University, D-55099 Mainz, Germany*

Georges Guiochon*

*Department of Chemistry, The University of Tennessee, Knoxville, Tennessee 37996-1600, and
Division of Chemical and Analytical Sciences, Oak Ridge National Laboratory,
Oak Ridge, Tennessee 37831*

Received August 27, 2002. In Final Form: November 14, 2002

Affinity distributions are calculated from adsorption isotherm data obtained for the enantiomers of L- and D-phenylalanine anilide (PA) on native and thermally annealed polymers molecularly imprinted with L-PA. The calculation is obtained with an iterative algorithm called expectation-maximization that does not require prior fit of the data to an isotherm model before inversion and thus yields a distribution indicative of the data only. The results show bimodal distributions, suggestive of a two-site model describing relatively selective and nonselective adsorption modes of the L-enantiomer and a corresponding unimodal/nonselective adsorption mode for the D-enantiomer. The nonselective adsorption region of the distributions exponentially decreases with increasing association constant, whereas the selective adsorption is Gaussian in appearance. The thermally annealed polymer exhibits altered affinity distributions that are somewhat less heterogeneous and more selective. Their selective sites have a lower saturation capacity than the native polymer. The capacity of the nonselective sites is inconclusive due to undersaturation of these lower energy sites, but it appears to be greater.

Introduction

The energetic or affinity distribution of solute adsorption on molecularly imprinted polymers (MIPs) is currently of interest as a tool in diagnosing the deleterious heterogeneity of these potentially useful adsorbents, which are advantageous due to their unique selectivity.^{1–5} The distribution function, $f(K) = \phi(\ln K)$, is most commonly convoluted with the Langmuir adsorption model to yield

the adsorption isotherm data obtained for study:

$$q(C) = \int \phi(\ln K) \frac{KC}{1 + KC} d(\ln K) = \int f(K) \frac{KC}{1 + KC} d(\ln K) \quad (1)$$

where $q(C)$ is the amount adsorbed in or on the surface of the polymer at equilibrium with a concentration C in the solution phase, and K is the association constant of the adsorption which is assumed to be distributed across a continuous range of values.

A common method of extracting $f(K)$ from eq 1 is to assume a form of the distribution function by differentiation of a smooth function describing the data. It is called an affinity spectrum (AS method). For the most general applicability, a cubic spline may be used to approximate the data.⁶ However, it has been shown that a more simple

* Corresponding author. Tel.: +1-865-974-0733. Fax: +1-865-974-2667. E-mail: guiochon@utk.edu.

(1) Umpleby, R. J., II; Bode, M.; Shimizu, K. D. *Analyst* **2000**, *125*, 1261.

(2) Umpleby, R. J., II; Rushton, G. T.; Shah, R. N.; Rampey, A. M.; Bradshaw, J. C.; Berch, J. K. Jr.; Shimizu, K. D. *Macromolecules* **2001**, *34*, 8446.

(3) Umpleby, R. J., II; Baxter, S. C.; Chen, Y.; Shah, R. N.; Shimizu, K. D. *Anal. Chem.* **2001**, *73*, 4584.

(4) Szabelski, P.; Kaczmarzski, K.; Cavazzini, A.; Chen, Y.-B.; Sellergren, B.; Guiochon, G. *J. Chromatogr. A* **2002**, *964*, 99.

(5) Whitcombe, M. J.; Rodriguez, M. E.; Villar, P.; Vulfson, E. N. *J. Am. Chem. Soc.* **1995**, *117*, 7105.

(6) Hunston, D. L. *Anal. Biochem.* **1975**, *63*, 99.

procedure is to utilize a Langmuir–Freundlich (LF) isotherm model, where the distribution is obtained from the parameters of the fit to this model analytically.³ The LF model yields a unimodal distribution of binding affinity with a central peak if the range of K values is adequately sampled in the isotherm data by

$$K'_{\min} = 1/C_{\max} \quad \text{and} \quad K'_{\max} = 1/C_{\min} \quad (2)$$

where K'_{\min} and K'_{\max} are the effective minimum and maximum K values in the distribution, and C_{\max} and C_{\min} are the maximum and minimum solution phase concentration values in the isotherm experiment. If the lower K side of the distribution is inadequately sampled by the maximum concentration values in the experiment, an exponentially decreasing function, beginning at K'_{\min} , is obtained. The Freundlich model yields an exponentially decreasing function regardless.⁷ Finally, note that in the study of liquid–solid equilibria, C_{\max} is often limited by the solubility of the compound studied in the solvent.

It has been argued that a unimodal distribution is the most appropriate assumption for MIP heterogeneity,³ although there are no compelling reasons for that. MIPs are polymers specifically designed to adsorb strongly one of the two enantiomers but it is physically impossible to avoid the nonselective adsorption of the compounds on their whole surface. In fact, Bilangmuir fits have often been used and have also been concluded by Scatchard plot analysis.^{8,9} In the distributed model this would suggest a bimodal distribution. To this point, no method of obtaining $f(K)$ has produced bimodal (or higher) distributions for MIPs. They have been calculated, however, with a numerical method for chromatographic stationary phases used in HPLC.^{10,11}

Analytical solutions for the distribution function obtained by differentiating smooth isotherm models has been accepted as preferable to numerical procedures, due to its simplicity.^{3,4} However, the utility of using a numerical procedure that does not imprint any shape or form on the distributions is undeniably important.⁷ They should be at least used to confirm the shape assumed in the other methods. With the numerical methods, the shape is dictated solely by the data.

In the distributions obtained for the chromatographic stationary phases,^{10,11} the experiments were conducted to probe active sites remaining after silanization. Bimodal or higher distributions were obtained. The active-site adsorption constant is sufficiently higher than the partitioning association constant that resolution between the two in the distribution function was easily obtained.

MIPs are imprinted for selective interaction with the solute molecule intended in the adsorptive application. In the separation of enantiomers, one of the pair is used for imprinting, and thus selective adsorption corresponding to a higher association constant is imparted to the polymer. Nonselective adsorption remains, produced by nonspecific interactions with various solutes, including both enantiomers. These may be general hydrophobic interactions, for example. It is these two types of interactions that have been modeled with bilangmuir isotherm equations.¹² The difference in association constants is often

around 2 orders of magnitude and so is the difference in saturation capacities. Correspondingly, the adsorption energy for the distinctly different mechanisms might be sufficiently different to be resolved by data analysis. Unfortunately, the AS method yields a unimodal peak width for a single-Langmuir isotherm (theoretically a delta-Dirac distribution function) that approaches a factor of 10 000 in association constant magnitude.³ With this type of resolution, it is virtually impossible to entertain the possibility of any type of distribution of affinity other than unimodal Gaussian, and this also limits the detection of homogeneity.

It remains highly plausible that MIPs imprinted for selective interactions may indeed display heterogeneity in two modes: one for the higher energy, selective association and one for the lower energy nonselective association. Improving MIP separation performance requires reducing the surface energetic heterogeneity. One approach is to decrease the nonselective adsorption, increase the selective adsorption capacity, and decrease the width of the selective adsorption heterogeneity that undoubtedly is produced by the imperfect imprinting process.²⁰

A higher resolution method for obtaining the affinity distribution is useful for deciphering the adsorption mechanism and optimizing the heterogeneity. It is also useful for validating other methods that impose a unimodal, exponential, or other shape on the distribution. Ample high quality data is required for this validation process. Due to the ill-conditioned nature of the inversion process used in solving eq 1, artifactual information in the distributions easily results from experimental errors present in the isotherm data.

We applied a purely numerical method to investigate the heterogeneity of a MIP imprinted for L-phenylalanine anilide (L-PA). Adsorption isotherms for both the L-PA and the D-PA isomers are analyzed in order to help justify the distributions obtained. The experiments were repeated at several temperatures. Although the position of the distributions may vary slightly, their shape should not change much with temperature in the rather narrow range investigated. Adsorption decreases with temperature, however, so different detected concentrations in the adsorbed phase as data are tested. The dependence of the saturation capacity of adsorbents as a function of temperature is not known well. Determining the saturation capacity from unsaturated data is fraught with sampling problems. Saturating a surface exclusively with a monolayer and with no solute–solute interactions (as assumed in the Langmuir local isotherm model) may not occur in practice.

Theoretical Section

Obtaining numerical estimates of affinity distributions requires an algorithm that inverts eq 1 to obtain $f(K)$ given only $q(C)$. Several methods have been proposed.^{7,13} We

(7) Jaroniec, M.; Madey, R. *Physical Adsorption on Heterogeneous Solids*; Elsevier: Amsterdam, 1988.

(8) Shea, K. J.; Spivak, D. A.; Sellergren, B. J. *J. Am. Chem. Soc.* **1993**, *115*, 3368.

(9) Sajonz, P.; Kele, M.; Zhong, G. M.; Sellergren, B.; Guiochon, G. *J. Chromatogr. A* **1998**, *810*, 1.

(10) Stanley, B. J.; Roy, A.; Krance, A. *J. Chromatogr. A* **1999**, *865*, 97.

(11) Stanley, B. J.; Krance, J. Submitted for publication.

(12) Gotmar, G.; Fornstedt, T.; Guiochon, G. *Anal. Chem.* **2000**, *72*, 3908.

(13) House, W. A.; Jaycock, M. J. *J. Colloid Polym. Sci.* **1978**, *256*, 52.

(14) Stanley, B. J.; Guiochon, G. *J. Phys. Chem.* **1993**, *97*, 8098.

(15) Stanley, B. J.; Guiochon, G. *Langmuir* **1994**, *10*, 4278.

(16) Stanley, B. J.; Bialkowski, S. E.; Marshall, D. B. *Anal. Chem.* **1993**, *65*, 259.

(17) Bialkowski, S. E. *J. Chemom.* **1991**, *52*, 11.

(18) Richardson, W. H. *Opt. Soc. Am.* **1972**, *62*, 55.

(19) Shepp, L. A.; Vardi, Y. *IEEE Trans. Med. Imag.* **1982**, *MI-2*, 113.

(20) Chen, Y.; Kele, M.; Sajonz, P.; Sellergren, B.; Guiochon, G. *Anal. Chem.* **1999**, *71*, 928.

have found an iterative maximum-likelihood method called expectation-maximization (EM) to be particularly stable and relatively free from artifacts as long as the data contains a minimum of errors, particularly systematic errors.^{14,15} This problem is general for any method used to obtain $f(K)$. We have observed, as a general rule, that the data fit improves with increasing resolution of the distribution. However, the risk incurred by modeling the errors in the data increases at the same time. This could result in artifactual peaks or in irrelevant information in the distribution increasing with resolution or quality of fit. The EM method appears to be a good compromise between resolution and stability.

The EM algorithm is attractive in its simplicity. Equation 1 is discretized as

$$q(C_i) = \sum_{j=K_{\min}}^{K_{\max}} f(K_j) \theta(C_i, K_j) \quad (3)$$

where

$$\theta(C_i, K_j) = \frac{K_j C_i}{1 + K_j C_i} \Delta(\ln K) \quad (4)$$

is the model kernel matrix defined for each solution phase concentration measured C_i and association constant in the distribution range K_j . $\Delta(\ln K)$ is the constant spacing between log K values in the discretized space. It is divided up logarithmically with input parameters for K_{\min} , K_{\max} , and the number of points to be calculated in the distribution.

An initial estimate for $f(K_j)$ is required which allows some flexibility in dictating the shape of the final distribution. However, we are interested in maximizing the influence of the data on the shape of the distribution. This requires a constant initial distribution:

$$f(K_j) = \frac{q_{\text{high}} - q_{\text{low}}}{\ln K_{\max} - \ln K_{\min}} \quad (5)$$

for all K_j . q_{high} and q_{low} are the highest and lowest measurements on the isotherm, respectively. In our studies, we have included (0,0) as the initial isotherm data point, and therefore $q_{\text{low}} = 0$. Equation 5 models the data range (numerator) evenly across the entire distribution range (denominator).

The isotherm is calculated q_{calc} with the estimate of $f(K)$ using eqs 3–4. The distribution is iteratively corrected by comparing the estimate at iteration k with the experimental isotherm data q_{exp} :

$$\alpha_i = q_{\text{exp}}(C_i) / q_{\text{calc}}(C_i) \quad (6)$$

Equation 6 produces a vector that corrects an estimate of the isotherm uniquely to yield the actual isotherm data. This vector is then convoluted with the model matrix to transform the isotherm correction into a distribution correction vector:

$$\beta_j = \sum_{i=1}^N \alpha_i \theta_{ij} \quad (7)$$

where N is the number of isotherm data points, and i and j are again the indices for concentration and association constant, respectively. To correct the distribution function,

$f(K)$ is multiplied by eq 7 at each K_j :

$$f(K_j)^k = \beta(K_j) f(K_j)^{k-1} \quad (8)$$

where $f(K)^{k-1}$ is the previous distribution estimate. Iteration proceeds by recalculating eqs 3, 6, 7, and 8 for each new estimate.

The EM algorithm is a general one for other types of data and models,^{16,17} and has been shown to proceed monotonically to the maximum-likelihood estimate for Poisson and Gaussian distributed data.^{18,19} Each step is guaranteed to converge. Note that zeros cannot be corrected in the algorithm; thus, if zeros are placed in the initial distribution they will stay that way and $q_{\text{calc}}(C=0)$ will always be zero (the fit is forced through zero if the initial point is (0,0)).

An attribute of the EM algorithm is that any range of K values may be investigated in the model for any concentration range. However eq 2 applies in that the distributions cannot be determined without support of data in the range bound by eq 2. In other words, if the data is not modeled well by the range of association constants input, a divergence at one or both ends of the distribution results, signaling that the appropriate K values are in a window below K_{\min} or above K_{\max} . The user must supply the appropriate K range to the algorithm, and supply data according to eq 2 to support this range. The benefit to observing a divergence (increasing values of $f(K)$) at an edge of the distribution is that one then has information that data exists in the isotherm better modeled beyond K_{\min} or K_{\max} . One can then either design an experiment to provide concentration values to support an extension of the window of association constants, or try to improve the analysis with the existing data by extending the end point(s) in order to deconvolute the poorly modeled information from the data that is well modeled within the window defined by eq 2. This latter point is an advantage, because one is not forced by the algorithm to model all of the data with a K range that may not actually account for all of the data in the system under study. The disadvantage is that the user must investigate this aspect in the data analysis and optimize K_{\min} and/or K_{\max} .

Experimental/Computational Section

The adsorption isotherms of L-phenylaniline anilide (L-PA) and D-phenylaniline (D-PA) anilide on an L-PA-imprinted copolymer were obtained at temperatures of 40, 50, 60, and 70 °C using the frontal analysis method of chromatography. They are described elsewhere.²⁰ A second set of experiments was performed on the polymer after annealing at 120 °C.

The affinity distributions were calculated with the expectation-maximization (EM) algorithm. Ten thousands iterations were performed across a range of 100 association constants K_i . No further improvement in the shape or resolution of the distributions was obtained with further iteration or number of association constants.

The effective range of association constants calculated by the algorithm, defined by the minimum and maximum concentration values in the mobile phase of the frontal analysis experiments, eq 2, are

$$K'_{\min} = 1/C_{\max} = (1.0 \text{ g/L})^{-1} = 1.0 \text{ L/g}$$

and

$$K'_{\max} = 1/C_{\min} = (5.0 \times 10^{-4} \text{ g/L})^{-1} = 2000 \text{ L/g}$$

As alluded to in the Theoretical Section, better isotherm fits are obtained by extending the low K end of the distribution K_{\min} to lower values: $K_{\min} < K'_{\min}$. This is illustrated in Figure 1 in

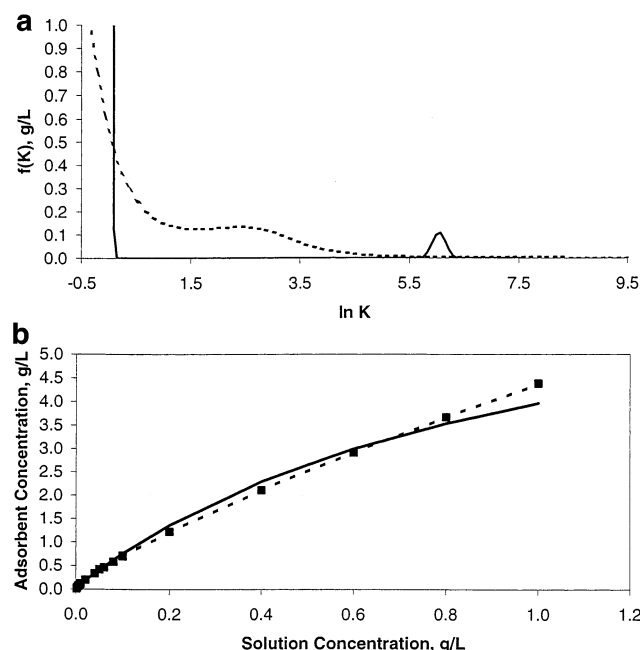


Figure 1. (a) Affinity distributions and (b) isotherm fits for L-PA on native polymer at 40 °C calculated with different K ranges. Solid line is the result obtained with the K range constrained by $K'_{\min} = 1$ L/g and $K'_{\max} = 2000$ L/g as defined by eq 2. Dashed line is the result obtained with the K range expanded to $K_{\min} = 0.01$ L/g and $K_{\max} = 20000$ L/g. Squares in (b) is experimental isotherm data.

which results are shown for $K = K'$ above and for an extend range with $K_{\min} = 0.01$ L/g and $K_{\max} = 20000$ L/g. The distributions are shown and the fits to the experimental data.

The effect is primarily a high-concentration one. Adsorption is still significantly increasing with concentration at C_{\max} , and unfortunately this concentration is 90–95% of the solubility of the isomers in the mobile phase and higher concentration data cannot be acquired. Constraining the K range to the K' range results in a poor fit of the data at high concentration values as shown in Figure 1b because these data is better modeled by K values $< K'_{\min}$. This suggests that a significant amount of adsorption is occurring with association constant(s) that are lower than can effectively be determined by the data. In the calculated distribution for the constrained calculation (solid line), a sharp divergence is observed at $K_{\min} = K'_{\min}$, which has been observed in many other data sets and calculations and is a very good indication of this general problem. In another study of the same data, the bilangmuir model was fit to the data, and $\ln K_1$ (symbolized b_1 in that publication) was -1.2 , which is out of the bounds of eq 2.

If K_{\min} is reduced one or 2 orders of magnitude below K'_{\min} a much better, indeed a very good fit to the data at high concentrations is obtained, suggesting further that this concentration range is best modeled with smaller association constants. However, a divergence at K_{\min} is still obtained. In separate studies, it has been shown that a nondivergent solution displaying a peak at low K can only be obtained if isotherm data is obtained to within 70% of the saturation capacity of the stationary phase,¹⁵ and it can be argued that this not only may be impractical but is probably impossible because of a theoretical breakdown in the Langmuir model.

The divergence at K_{\min} for the expanded range calculation is not as sharp. It appears as an exponentially decreasing solution with increasing K . This is a result reported with alternate methods of calculating the distribution, and is the theoretical result obtained with a Freundlich isotherm.⁴ There is also an effect on the distribution at higher association constants. Under constrained conditions, the distribution is sharply divergent at $K_{\min} = K'_{\min}$ and a small peak picks up the higher K association contained in the isotherm data. Under unconstrained conditions the exponentially decreasing solution at K_{\min} or K'_{\min} displays a shoulder at intermediate K values, with further information

possible at higher K . It is important to note that further reduction in K_{\min} does not alter the distribution between K'_{\min} and K'_{\max} significantly. It appears with this procedure that low K information is successively deconvoluted from the effective K' range, and thus the distribution within this range is more consistently and accurately modeled by not forcing a calculation with K values unrepresentative of the data.

Therefore the procedure followed in the calculation of the affinity distributions is to calculate under constrained conditions, expand the end points 1 order of magnitude, then 2, until no significant change in the distribution between K'_{\min} and K'_{\max} is obtained and no further. As shown here, this typically results in 1–2 factors of 10 below K'_{\min} . The effect with K_{\max} is much less, since much less adsorption is typically observed at very high association constants. Usually this procedure only need be repeated for a few data sets within an entire system of data to find appropriate K_{\min} and K_{\max} values that will yield consistent results across all of the data sets. For the current study, $K_{\min} = 0.01$ L/g and $K_{\max} = 20,000$ L/g was applied to all calculations of the affinity distributions.

It is important to note that although the distributions are calculated with the above end points, they should only be interpreted physicochemically within K'_{\min} and K'_{\max} . Therefore, in the distribution plots that follow, only this “effective” range is displayed.

The effect of this procedure to calculate the distributions is that a substantial amount of the range of isotherm data (the high concentration range) is not effectively modeled, and that the total saturation capacity of the polymer is not estimated well. The problem of estimating the total saturation capacity was also noted in other studies,⁴ so this is not an artifact of the EM method. For the purposes of interpretation, then, only the saturation capacity of the polymer obtained by summing the differential capacities within K'_{\min} and K'_{\max} was performed:

$$q_s = \sum_i f(K_i) \Delta(\ln K) \quad (9)$$

where the sum is over any range of interest within the effectively modeled range, and $f(K_i)$ is the distribution function at point i and $\Delta(\ln K)$ is the spacing between points in the distribution.

Results and Discussion

The distribution functions for D-PA and L-PA obtained at the four different temperatures are shown in Figure 2 for the native polymer and Figure 3 for the annealed polymer. Adsorption decreases with temperature as evident from the ordinate scales. The general shape of the distributions does not change with temperature, however, as expected, due to the narrow range investigated. This consistency is a figure of merit for the method.

In all of the distributions, it is apparent that a substantial amount of adsorption in the region defined by $\ln K = 1.5$ and $\ln K = 4.5$ exists for L-PA relative to D-PA. It may therefore be concluded that adsorption in this region is selective for L-PA and is a result of specific enantiomeric interactions. On the other hand, the distributions tend to diverge to high values of $f(K)$ at K'_{\min} for both enantiomers. This is to be expected. Selective and nonselective adsorption sites have been modeled previously with the bilangmuir isotherm with substantially less adsorption (saturation capacity) at the selective site occurring for the less retained member of the enantiomeric pair in chiral separations.^{12,20} The mean or value of K at the maximum in the distributions for the specific interactions is similar to the values obtained for K_2 by the bilangmuir model. However, in publications introducing the general methodology of determining affinity distributions for molecularly imprinted polymers, only exponentially decreasing or unimodal distributions have been calculated (AS method).^{1–5} The EM method of calculating affinity dis-

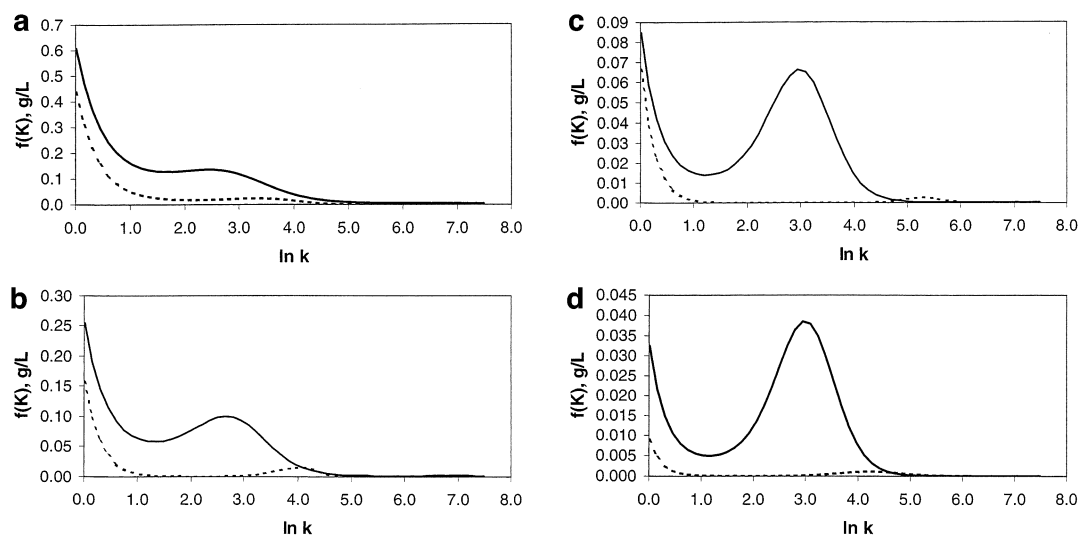


Figure 2. Affinity distributions of L-PA (solid curve) and D-PA (dashed curve) on native polymer at (a) 40 °C, (b) 50 °C, (c) 60 °C, and (d) 70 °C.

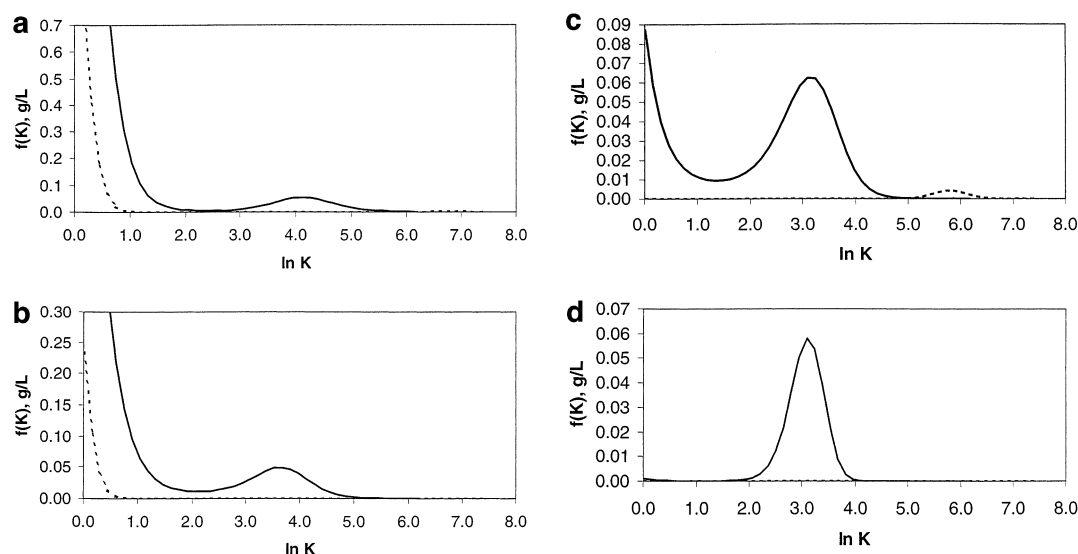


Figure 3. Affinity distributions of L-PA (solid curve) and D-PA (dashed curve) on annealed polymer at (a) 40 °C, (b) 50 °C, (c) 60 °C, and (d) 70 °C.

tributions appears to produce a hybrid of these distinctly different, alternate methods.

The AS method uses either cubic spline, Freundlich, or Langmuir–Freundlich isotherm model fits and a distribution function derived from these functions with a first or second-order finite difference approximation. The cubic spline allows the greatest flexibility in obtaining the general shape of the distribution as defined by the data; the Freundlich isotherm yields an exponentially decreasing distribution function; and the Langmuir–Freundlich isotherm yields either an exponentially decreasing function or a unimodal distribution with a peak maximum. For similar systems, Scatchard plot and bilangmuir analysis indicates that a two-site model represents the data. The distributions reported in this contribution are the first that show that a two-site or bimodal model is indeed indicative of the data, using the general methodology of isotherm inversion to yield an affinity distribution. These results suggest that the EM method has greater resolution than the AS method.

The exponentially decreasing, low K end of the distributions is more nonselective in nature since it is detected for both L-PA and D-PA. However it is not exclusively

nonselective, since adsorption in this region is still greater for L-PA than for D-PA. This suggests that some enantiomeric-selective mechanism may be operative in the “nonselective” adsorption sites. In AS computations on the same data at 70 °C, exponentially decreasing functions are obtained by use of the Freundlich isotherm model and less amplitude is also observed beginning at K'_{\min} . However, the AS distributions decay similarly to $\ln K \approx 4$ for each isomer, suggesting that the total capacity is reduced for D-PA across the entire K range, but the relative contributions of high and low K adsorption remains similar. The heterogeneity parameter from the Freundlich model is 0.90 vs 0.96 for L-PA vs D-PA on the native polymer and 0.94 vs 0.99 for the same comparison on the annealed polymer. The EM distributions attribute the differences more selectively to the most probable regions of the distribution.

Thermal annealing was performed with the hypothesis that heterogeneity would be decreased. An effect on the distributions was noted, however the effect was not constant across the different-temperature isotherms measured. At 40 and 50 °C, the effect was increased adsorption toward K'_{\min} and decreased adsorption between

Table 1. Results of Adsorption Distribution Analysis^a

Native						
temp (°C)	$q_{\text{high,exp}}$	$q_{\text{s,t}}^*$	$q'_{\text{s,t}}$	$q_{1,\text{t}}$	$\ln K_{2,\text{max}}$	$q_{\text{s},2}$
40	4.38, 3.91	62.2, 60.6	0.734, 0.280	0.430, 0.224	2.6, 3.3	0.303, 0.0556
50	3.17, 2.74	53.1, 40.4	0.362, 0.0744	0.171, 0.0585	2.8, 4.1	0.188, 0.0159
60	2.38, 2.05	47.0, 38.8	0.155, 0.0249	0.049, 0.0225	3.0, 5.3	0.106, 0.0025
70	1.86, 1.64	41.2, 36.2	0.075, 0.0047	0.018, 0.0028	3.0, 4.2	0.058, 0.0019
Annealed						
temperature (°C)	$q_{\text{high,exp}}$	$q_{\text{s,t}}^*$	$q'_{\text{s,t}}$	$q_{1,\text{t}}$	$\ln K_{2,\text{max}}$	$q_{\text{s},2}$
40	5.24, 4.68	33.4, 34.0	1.65, 0.444	1.55, 0.441	4.0, 6.8	0.093, 0.0022
50	3.93, 3.55	42.6, 43.0	0.534, 0.0583	0.453, 0.0583	3.6, <i>b</i>	0.081, <i>c</i>
60	2.90, 2.55	58.9, 77.6	0.134, 0.0036	0.044, <i>c</i>	3.2, 6.0	0.089, 0.0036
70	2.21, 1.99	66.3, 73.9	0.0465, <i>c</i>	0.0004, <i>c</i>	3.0, <i>c</i>	0.046, <i>c</i>

^a Symbols are defined in text. Values are represented as (L-PA, D-PA), i.e., the corresponding values for L-PA first, followed by D-PA.

^b Slight divergence at K_{max} observed; therefore, $K_{2,\text{max}} > K'_{\text{max}}$. ^c Capacity less than 1×10^{-4} g/L (less than detection limit).

$\ln K \approx 1$ and $\ln K \approx 3$ for the annealed polymer with respect to the native polymer, suggesting decreased heterogeneity of selective adsorption. However, this is accompanied by decreased saturation capacity of the “selective” sites. At 60 °C and 70 °C, decreased heterogeneity of the selective site was also observed; but the capacity of the unselective sites for the annealed polymer did not increase as determined at 40 °C and 50 °C (this was also observed with the AS method at 70 °C⁴). However, remember that $K_{\text{min}} < K'_{\text{min}}$ in the EM method. The high concentration data is ineffectively modeled at lower association constants not shown in the plots for the annealed polymer at 60 °C and especially 70 °C.

The D-PA distributions for the annealed polymer displayed decreased adsorption in both regions except at 60 °C for the high K site (this was also observed with the AS method at 70 °C⁴). Most of the adsorption is best modeled by $K < K'_{\text{min}}$.

Due to the bimodal and apparent selective and unselective nature of the distributions, the differential sorption capacities were summed in different regions and the following is defined:

$q_{\text{high,exp}}$, experimental amount of adsorption at highest concentration measured;

$q_{\text{s,t}}^*$, sum of differential capacities of entire calculated distribution;

$q'_{\text{s,t}}$, sum of differential capacities across effectively modeled K' range;

$q_{\text{s},1}$, sum from $\ln K'_{\text{min}} = 0$ to $\ln K = 1.5$, “nonselective” or nonspecific adsorption; and

$q_{\text{s},2}$, sum from $\ln K = 1.5$ to $\ln K'_{\text{max}} = 7.6$, “selective” or specific adsorption.

The results for both isomers and polymers are reported in Table 1. $q_{\text{s,t}}^*$ is the total saturation capacity of the polymer as determined by the EM method. The majority of this exists at $K < K'_{\text{min}}$ and is therefore an inaccurate estimate. Compared to the values obtained with the bilangmuir isotherm,²⁰ they are overestimated. For every isotherm case studied, the annealed polymer displayed greater total adsorption, $q_{\text{high,exp}}$. However, this is not always the case in the estimated $q_{\text{s,t}}^*$ values.

The sum saturation capacity in the effective K' range $q'_{\text{s,t}}$ is substantially less than the total adsorption observed because of the ineffectively modeled high concentration region as discussed previously. The amount of adsorption effectively modeled $q'_{\text{s,t}}$ as a percentage of the total amount observed is plotted in Figure 4. A decrease with temperature is observed and this is due to more adsorption being modeled between K_{min} and K'_{min} as temperature increases. This suggests that the nonselective association constant(s) decrease with increasing temperature. This was also

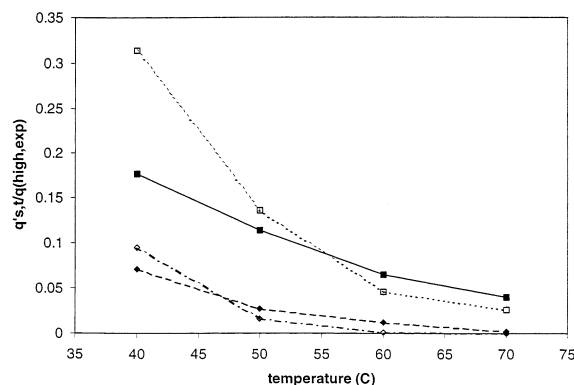


Figure 4. Fraction of total adsorption observed that is modeled effectively in K' range for (solid line, solid squares) L-PA on native polymer, (dashed line, solid diamonds) D-PA on native polymer, (dotted line, open squares) L-PA on annealed polymer, and (dotted-dashed line, open diamonds) D-PA on annealed polymer.

observed with the bilangmuir model.²⁰ With an exponentially decreasing distribution function, this would result in less adsorption above K'_{min} as temperature is increased. The effect is greater for the annealed polymer. The plots also show that there is substantially less adsorption in the effectively sampled K' range for the D-isomer, because less adsorption at association constants greater than one is present.

The mean selective affinity constant K_2 appears to increase with temperature for both enantiomers on the native polymer. K_2 appears to decrease with temperature for L-PA on the annealed polymer, and no dependence is observed for D-PA. Since the selective adsorption is relatively much less for D-PA than for L-PA (especially for the annealed polymer), the relative error of the adsorption in this region is suspected to be much greater.

The fractional saturation capacities of the selective and unselective sites for the native and annealed polymers are plotted with temperature in Figures 5 and 6. The decrease with temperature for the unselective site (Figure 5) is greatest for the annealed polymer (both isomers) because the amount modeled below K'_{min} increases the greatest with temperature in this case (Figure 4, Table 1). Taken together, $q_{\text{s},1}$ and $q_{\text{high,exp}} - q_{\text{s},2}$ or $q_{\text{s,t}}^* - q_{\text{s},2}$ are interpreted as the nonselective adsorption. Unfortunately, $q_{\text{high,exp}}$ varies from experiment to experiment, and $q_{\text{s,t}}^*$ is inaccurate, so an accurate estimation of the saturation capacity of nonselective adsorption is not possible with this method.

The saturation capacity of the higher K selective adsorption, however, is accurately determined. Figure 6

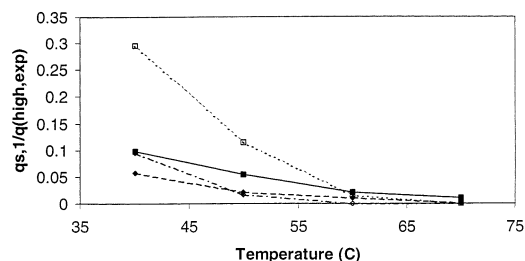


Figure 5. Fraction of total adsorption observed experimentally that is modeled as nonselective or nonspecific adsorption. (solid line, solid squares) L-PA on native polymer, (dashed line, solid diamonds) D-PA on annealed polymer, (dotted line, open squares) L-PA on annealed polymer, and (dashed–dotted line, open diamonds) D-PA on annealed polymer.

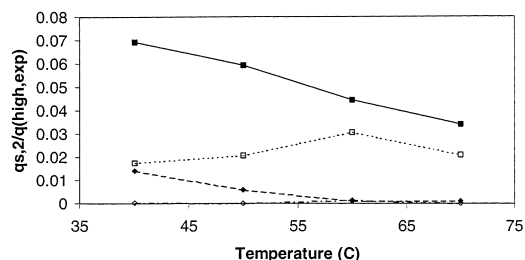


Figure 6. Fraction of total adsorption observed experimentally that is modeled as selective or specific adsorption. (solid line, solid squares) L-PA on native polymer, (dashed line, solid diamonds) D-PA on annealed polymer, (dotted line, open squares) L-PA on annealed polymer, and (dashed–dotted line, open diamonds) D-PA on annealed polymer.

Table 2. Selectivity of L-PA over D-PA for Unspecific and Specific Interactions Determined through Adsorption Distribution Analysis

temp (°C)	native		annealed	
	unspecific	specific	unspecific	specific
40	0.98	5.4	0.98	42.3
50	1.31	11.8	0.99	8100
60	1.21	42.9	0.76	24.7
70	1.14	30.3	0.90	575

shows that the selective capacity of the annealed polymer is lower than that of the native polymer (regardless of the temperature of the experiment). This is true for L-PA which displays most of the selective adsorption, not for D-PA.

The selectivity for L-PA over D-PA was calculated as

$$\alpha_U = (q_{s,t}^* - q_2)_{L-PA} / (q_{s,t}^* - q_2)_{D-PA} \quad \text{"unspecific" selectivity}$$

$$\alpha_S = (q_2)_{L-PA} / (q_2)_{D-PA} \quad \text{"specific" selectivity}$$

and is reported in Table 2. The selectivity of the "unspecific" site is seen to have values close to one in all cases, and this agrees well with the bilangmuir model.²⁰ The

native polymer is more selective for L-PA than the annealed polymer at these sites, the latter displays selectivities less than one in each case—suggesting that the annealed polymer's unselective adsorption may be slightly more selective for D-PA than to L-PA (this was not observed with the bilangmuir model). For the "specific" site, the values are substantially greater for both polymers (as observed with the bilangmuir model), with the annealed polymer showing greater values for three out of four experiments (not observed with the bilangmuir model). This comparison was not possible with the AS method since there is no resolution between the different types of adsorption.

Conclusion

Affinity distributions of adsorption on an enantioselective MIPs are bimodal in nature, with one region corresponding to selective or specific adsorption, exhibiting a high association constant relative to the other region in which smaller unselective or nonspecific association constants exist. The specific adsorption is due to the tailored interactions from imprinting the polymer with the L-isomer. The unselective adsorption is due to nonselective interactions, mostly hydrophobic. These latter adsorption constants and their corresponding saturation capacities are not determined well by the method, for the lack of high concentration data that maps out the adsorption model in this region. Most of the adsorption of the molecularly imprinted polymers studied is modeled as unselective adsorption. Annealing the polymers modestly decreases the heterogeneity or dispersion of the distributions and increases the selectivity in the specific higher K region, however the saturation capacity in this region decreases. The saturation capacity of the unselective adsorption increases with annealing, although this is concluded by inspection of the experimentally determined total adsorption, not the modeled total saturation capacity that is inaccurate.

Chromatographically, our results predict for L-PA that band tailing should be less and that the separation should be greater with the annealed polymer as long as the smaller saturation capacity of the annealed polymer at the selective sites is not surpassed. If it is, the band fronts obtained with the annealed stationary phase will shift toward lower t_R more rapidly. The decreased saturation capacity may not be advantageous for preparative chromatography.

Acknowledgment. This work was supported in part by Grant DE-FG05-88-ER-13869 of the US Department of Energy and by the cooperative agreement between the University of Tennessee and the Oak Ridge National Laboratory. B.J.S. acknowledges the donors of the Petroleum Research Fund administered by the American Chemical Society for funding at CSUSB.

LA020747Y